tions further showed that for angles near 40° incidence to the water surface, vertically polarized radiometric temperatures are invariant with changes in sea state (Fig. 5, left side). Furthermore, it has been shown that the radiometric temperature is nearly insensitive to changes in the water thermometric temperature near the water resonance line (Fig. 5, right side). A frequency of 30 GHz was selected since the radiometric temperature is still essentially invariant to water temperature and at a frequency within an atmospheric window. It has been determined that any deviation from radiometric temperature invariance can be corrected by means of iterative computations.

In summary, the basis for performing sea state and sea temperature measurements using selected dual frequencies and orthogonal polarizations are 1) horizontally polarized microwave radiometric signals are significantly sensitive to changes in sea state and incidence angle (and in a lesser way to sea temperature); 2) vertically polarized microwave radiometric signals are invariant to sea state at or near an incidence angle of 40° to the surface; 3) microwave radiometric signals (of both polarizations) are nearly invariant to changes in the water thermometric temperature at frequencies at or near that of water absorption; and 4) the effects of nonpolarized loss mechanisms, like intervening atmosphere and foam, can be removed.

The method of removing the effects of non-polarized loss mechanisms that has been proposed by Aukland[4] et al. relies on the ability to generate a set of simultaneous equations with variables that are dependent on the sea state and parameters that are independent of the sea state. Solving these set of equations in effect allows the sea state conditions to be determined without overtly evaluating the attenuation contributed by the intervening atmosphere.

In a practical situation a curve will be generated relating radiometric attenuation. This in turn allows the data reduction process to be a simple set of tables on which values may be determined by direct "look-up." The nature of the sea is such that abrupt changes in sea state are rarely encountered. This fact in turn indicates that previous values of sea state can be used as a starting point in the search for the next value, further simplifing the data processing problem.

This technique of sea state measurement has been recently proposed with the result that considerable interest has been shown by the remote sensing community.

Summary

This paper treats the effect of the atmosphere on passive microwave remote sensing in a general summary nature. No attempt has been made to present an exhaustive technical treatment of the mechanisms involved in the atmospheric effects, nor to catalogue all of the possible applications related to this method of remote sensing. Recently, several special issues of technical journals have contained excellent treatises on these topics. Specfic reference is made to *Proceedings of the IEEE* special issue on Remote Environmental Sensing, April, 1969; *IEEE Transactions on Microwave Theory and Techniques* special issue on Noise, September, 1968 and *Proceedings of Symposium on the Remote Sensing of the Environment* sponsored by the University of Michigan.

References

[1] Staelin, D. H., "Passive Remote Sensing at Microwave Wavelengths," *Proceedings of the IEEE*, Vol. 57, April 1969, p. 427.

[2] Kreiss, W. T., "The Influence of Clouds on Microwave Brightness Temperatures Viewing Downwards Over Open Seas," *Proceedings of the IEEE*, Vol. 57, April 1969, p. 440.

[3] Stogryn, A., "The Apparent Temperature of the Sea at Microwave Frequencies," *IEEE Transactions on Antennas and Propogation*, Vol. AP-15, 1969, p. 278.

[4] Aukland, J. C. et al., "Remote Sensing of the Sea Conditions with Microwave Radiometer System," *Sixth Symposium on Remote Sensing of Environment*, Univ. of Michigan, Oct. 1969.

Subsonic-Hypersonic Aerodynamic Characteristics of Several Bodies of Revolution

Amado A. Trujillo*
Sandia Laboratories, Albuquerque, N. Mex.

Nomenclature

C_{AA} = forebody drag coefficient
$C_{N\alpha}$ = slope of normal force coefficient near $\alpha = 0°$, 1/deg
CP = fraction of model length from model nose to center of pressure
R = freestream Reynolds number based on model length
α = model angle of attack, deg

INTEREST in the aerodynamic characteristics of low-drag, high-volume re-entry vehicles, coupled with the paucity of this information for shapes other than cones, led to a series[1] of experimental and theoretical programs which sought to define drag, normal force, and static stability. The purpose of this Note is to summarize this work for four of these re-entry vehicle shapes. Sketches of the four fineness ratio 3 models, together with equations defining the model shapes, are shown in Fig. 1.

In 1952, Dennis and Cunningham[2] conducted tests at NACA on $\frac{1}{2}$- and $\frac{3}{4}$-power-law bodies and conical shapes with varying fineness ratios over a supersonic range of Mach numbers. More recently, Browne[3] tested $\frac{3}{4}$-power-law shapes with varying degrees of nose bluntness over the hypersonic Mach number range. At about the same time, Pousma[4] and Trujillo[5] of Sandia Laboratories tested seven configurations including $\frac{3}{4}$-power-law shapes with variations in nose bluntness, base corner rounding, and fineness ratio, as well as $\frac{1}{2}$-power-law, parabolic, and L-V Haack shapes. These tests were carried out over a range of Mach numbers from subsonic to hypersonic.

Theoretical studies on the configurations investigated experimentally by Pousma and Trujillo were carried out by Berman, et al.[6] and Franks.[7] Berman used an "exact" solution, while Franks used an "approximate" solution in calculating the aerodynamic characteristics. In addition, predictions were made using Newtonian impact theory.[8] Berman used the General Electric numerical flowfield solution. The solution in the nose region of a blunt body was carried out by direct transonic solution utilizing a streamline stepping technique in which computed shock wave shapes and body pressure distributions were compared with initially assumed values. A steady-state solution was carried out in the supersonic region, using the method of characteristics for both the pointed and blunt-nosed bodies. Franks' calculations were based upon a linearized method of characteristics program modified to accept the analytic descriptions of the models. In addition, he used other programs including blunt-body and conical-flow procedures to obtain initial-value data for the linearized method of characteristics program as well as aiding in the calculation of the geometric parameters required for the analytic body descriptions.

The experimentally and theoretically determined variations of $C_{N\alpha}$ and CP with Mach number for α near zero degree are presented in Fig. 1. For the configurations studied, the "exact" theory of Berman most accurately predicted the static stability coefficients. It is of interest to note that the Newtonian impact theory does offer a simple, and reasonably accurate, means of calculating the static stability of axisymmetric vehicles at hypersonic Mach numbers.

Received March 16, 1970; revision received May 25, 1970. This work was supported by the U.S. Atomic Energy Commission.

* Staff Member, Experimental Aerodynamics Division, Aerothermodynamics Projects Department. Member AIAA.

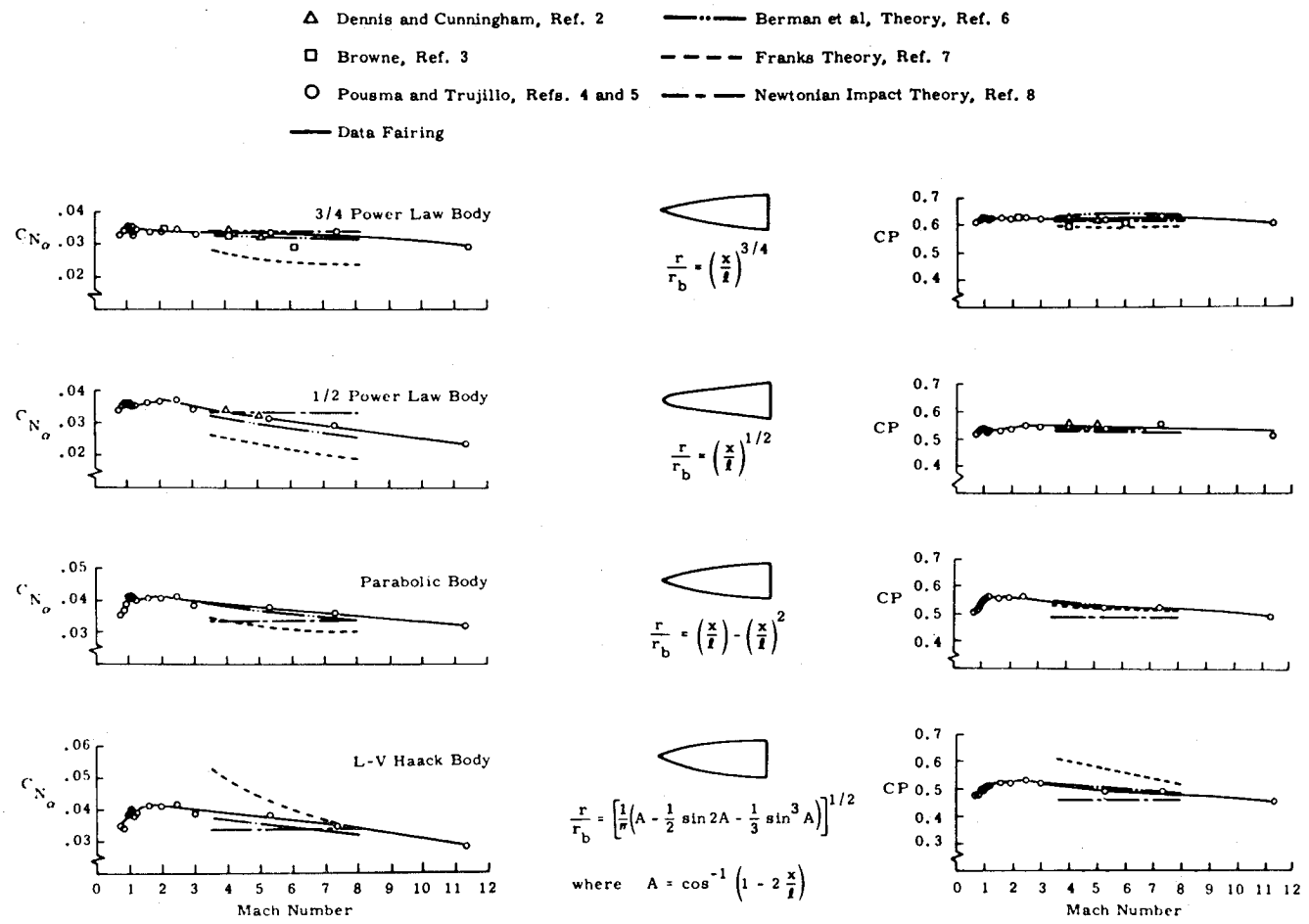

Fig. 1 Static stability characteristics and equations defining model shapes for the four fineness ratio 3 models investigated.

The experimentally determined zero degree angle-of-attack forebody drag data (wave plus skin-friction drag) for the Mach number range 4.0 to 11.4 are presented as functions of Reynolds number in Fig. 2. Base drag was eliminated because geometric similarity of the sting-body combination was not maintained at the different facilities. For the range of Reynolds numbers considered, variations as large as 70% in forebody drag coefficient are possible. Variations of this magnitude emphasize the need to use care in properly interpreting forebody drag data for application to full-scale vehicle flight conditions.

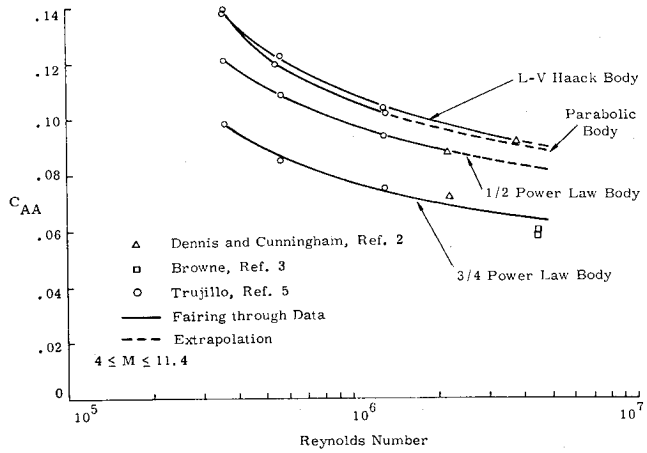

Fig. 2 Variation of forebody drag coefficient with Reynolds number.

References

[1] Trujillo, A. A., "Summary of Static Stability and Drag Characteristics of Axisymmetric Low-Drag Shapes for the Subsonic to Hypersonic Mach Number Range," SC-RR-68-304, Aug. 1968, Sandia Labs., Albuquerque, N. Mex.

[2] Dennis, D. H. and Cunningham, B. E., "Forces and Moments on Pointed and Blunt Nosed Bodies of Revolution at Mach Numbers from 2.75 to 5.00," RM A52E22, Aug. 1952, NACA.

[3] Browne, P. D., "Results of Wind Tunnel Program in AEDC Tunnel A to Obtain Static Stability and Drag Data on a $\frac{3}{4}$ Power Law Body in Support of the CRESS Program," Aerodynamics Technology Component Data Memo ATDM 65-17, Nov. 1965, General Electric Co.

[4] Pousma, J. G., "Static Stability and Axial Force Test of N-Power Bodies at Mach 0.7 to Mach 3.0," SC-TM-65-564, Sept. 1966, Sandia Labs., Albuquerque, N. Mex.

[5] Trujillo, A. A., "Static Stability and Axial Force Test of Seven N-Power Bodies at Mach Numbers of 5.3, 7.3, and 11.4," SC-TM-65-563, Sept. 1966, Sandia Labs., Albuquerque, N. Mex.

[6] Berman, R. J. et al., "Aerodynamic Characteristics Study," Document 66SD664A, April 1966, General Electric Co.

[7] Franks, W. J., "Aerodynamic Coefficients of Seven Lifting Bodies of Revolution Near Zero Angle of Attack at Mach Numbers of 3.5, 5, and 8," NOR-66-205, May 1966, Northrop Corp.

[8] Stoller, H. M. and Lathrop, J. F., "A Modified Newtonian Theory Program (MONET) for Calculating Aerodynamic Coefficients," SCL-DR-65-139, March 1966, Sandia Labs., Livermore, Calif.